

Physarum Multi-Commodity Flow Dynamics

Vincenzo Bonifaci¹, Enrico Facca², Frederic Folz³,
Andreas Karrenbauer⁴, Pavel Kolev⁴, Kurt Mehlhorn⁴,
Giovanna Morigi³, Golnoosh Shahkarami⁵, and Quentin Vermande⁶

¹*Dipartimento di Matematica e Fisica, Università degli Studi Roma Tre, Roma, Italy*

²*Scuola Normale Superiore, Pisa, Italy*

³*Fachbereich Physik, Universität des Saarlandes, Saarbrücken, Germany*

⁴*Max Planck Institute for Informatics, Saarbrücken, Germany*

⁵*Max Planck Institute for Informatics and Fachbereich Informatik, Universität des Saarlandes*

⁶*École Normale Supérieure, Paris, France*

September 24, 2020

Abstract

In wet-lab experiments [NYT00, TTS⁺10], the slime mold *Physarum polycephalum* has demonstrated its ability to solve shortest path problems and to design efficient networks, see Figure 1 for illustrations. *Physarum polycephalum* is a slime mold in the Mycetozoa group. For the shortest path problem, a mathematical model for the evolution of the slime was proposed in [TKN07] and its biological relevance was argued. The model was shown to solve shortest path problems, first in computer simulations and then by mathematical proof. It was later shown that the slime mold dynamics can solve more general linear programs and that many variants of the dynamics have similar convergence behavior. In this paper, we introduce a dynamics for the network design problem. We formulate network design as the problem of constructing a network that efficiently supports a multi-commodity flow problem. We investigate the dynamics in computer simulations and analytically. The simulations show that the dynamics is able to construct efficient and elegant networks. In the theoretical part we show that the dynamics minimizes an objective combining the cost of the network and the cost of routing the demands through the network. We also give alternative characterization of the optimum solution.

Contents

1	Introduction	2
2	Case Studies	7
2.1	Multi-commodity Flow in a Ring	7
2.1.1	Two Edge Solution	7
2.1.2	Three Edge Solution	7
2.1.3	Computer Simulations	8
2.2	The Bow-Tie Graph	8
2.3	A Case Study Inspired by [TTS ⁺ 10]	9
3	Preliminaries	10
4	Existence of a Solution	13
5	Fixed Points	14

6	Lyapunov Function	14
7	Further Properties of the Lyapunov Minimum	15
8	Convergence to the Lyapunov Minimizer	18
9	A Connection to Mirror Descent	19
10	Conclusions	21

1 Introduction

In wet-lab experiments [NYT00, TTS⁺10], the slime mold *Physarum polycephalum* was shown to solve shortest path problems and to design efficient networks, see Figure 1 for illustrations. *Physarum polycephalum* is a slime mold in the Mycetozoa group [BD97]. Its cells can grow to considerable size (of a human hand) and it can form networks.

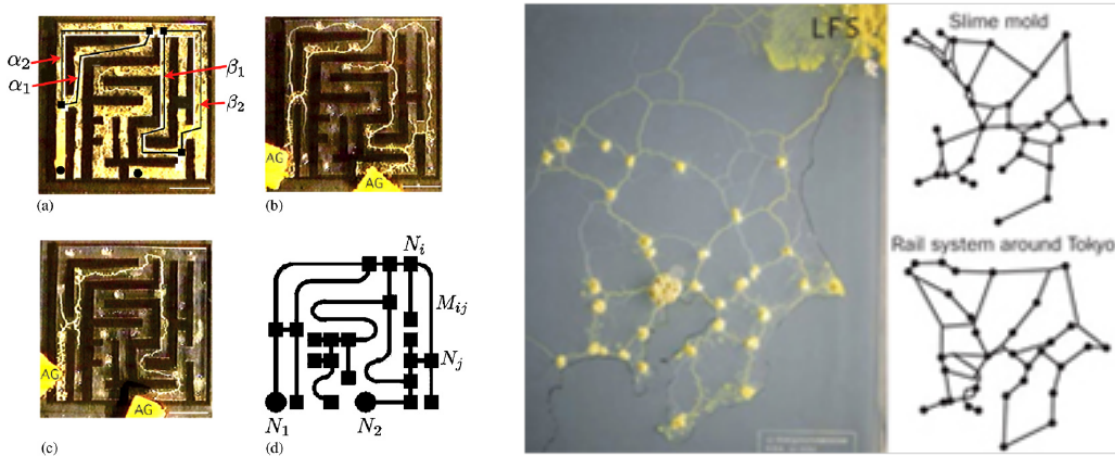


Figure 1: The figure on the left shows the shortest path experiment. It is reprinted from [NYT00]. The edges of a graph were uniformly covered with *Physarum* (subfigure (a)) and food in the form of oat-meal was provided at the locations labeled AG in subfigure (b). After a while the slime retracted to the shortest path connecting the two food source (subfigure (c)). The underlying graph is shown in (d).

The figure on the right shows the network design experiment. It is reprinted from [TTS⁺10]. Food was provided at many places (the larger dots in the picture) and the slime was constrained to live in an area that looks similar to the greater Tokyo region. The large dot in the center corresponds to Tokyo and the empty region below it corresponds to Tokyo bay. The slime formed a network connecting the food sources. The two graphs on the right compare the network built by the slime with the railroad network in the Tokyo region.

A theoretical explanation is available for the shortest path problem. In [TKN07] a mathematical model in the form of a coupled system of differential equations was given for modeling the evolution of the slime, the biological relevance of the model was argued, and the model was shown to solve shortest path problems in computer simulations. Proofs that the model solves shortest path problems can be found in [BMV12, Bon13, KKM20]. The *Physarum* dynamics is also able to solve more general linear programs [SV16a, SV16b, IJNT11, KKM20].

Tero, Kobayashi and Nakagaki [TKN07] model the slime network as an electrical network $G = (V, E)$ with time varying resistors. Each edge e of the network has a fixed positive length c_e and a time-varying diameter $x_e(t)$. In this paper, we will refer to c_e as the cost of the edge and to

x_e as the capacity of the edge. The resistance of e at time t is then $r_e(t) = c_e/x_e(t)$. Let s_0 and s_1 be two fixed vertices in the network. One unit of current is sent from s_0 to s_1 . Let $q_e(t)$ be the current flowing across e . Then the capacity of e evolves according to the differential equation

$$\dot{x}_e = \frac{d}{dt}x_e(t) = |q_e| - x_e \quad \text{for all } e \in E.$$

As is customary, we write \dot{x} for the derivative with respect to time and drop the time-argument of x and q . Tero et al. showed in computer simulations that a discretization of the model converges to the shortest path connecting the source and the sink, i.e., $x_e(\infty) = 1$ for the edges on the shortest path and $x_e(\infty) = 0$ for the other edges. This assumes that the shortest path is unique. Bonifaci et al. [BMV12] proved convergence. In the limit $t \rightarrow \infty$ (in equilibrium), we have $x_e = |q_e|$ for all e , i.e., the electrical flow through an edge is equal to the capacity of the edge.

No theoretical explanation is yet available for the network design experiment, i.e., there is no biologically plausible model¹ that constructs in computer simulations networks similar to the networks constructed by Physarum Polycephalum. We introduce a model that generalizes the model in [TKN07], analyze its theoretical properties, in particular show convergence of the dynamics and characterize the limit for $t \rightarrow \infty$, and show in computer experiments that it constructs *nice* networks. We do not argue biological plausibility.

The shortest path problem can be viewed as a network design problem. Given two vertices in a graph, the goal is to construct the cheapest network connecting the given vertices. The solution is the shortest path connecting the given vertices. The shortest path problem can also be viewed as a minimum cost flow problem. We want to send one unit of flow between the given vertices and the cost of sending a certain amount across an edge is equal to the cost of the edge times the amount sent. The solution is the shortest path connecting the given vertices.

Networks are designed for a particular purpose. For this paper, the purpose is multi-commodity flow. Suppose that we have many pairs of vertices between which we want to send flow. We want to construct a network that satisfies the many demands in an economical way. Economical could mean many things: minimum cost of the network (that's the Steiner tree problem), shortest realization of each demand (then the network is the union of the shortest paths), or something in the middle, i.e., some combination of total cost of the network and the cost of routing the demands in the network. We assume that there is some benefit in sharing a connection, i.e., the cost of sending one unit each of two commodities across an edge is lower than two times the cost of sending one unit of one commodity across the edge.

Our model for the multi-commodity network design problem is inspired by the Physarum model for the shortest path problem. Let $A \in \mathbb{R}^{n \times m}$ be an arbitrary real matrix² and let b_1 to b_k in \mathbb{R}^n be k right-hand sides for the linear system $Af = b$.

Assumption 1. *We assume $b_i \in \text{Im}A$ for $1 \leq i \leq k$, i.e., the linear systems $Af = b_i$ are feasible.*

We refer to the columns of A as edges and the rows of A as nodes, use e, e' to index columns and v and w to index rows of A . The e -th column of A is denoted A_e . Each edge e has a positive cost c_e and a (time-varying) capacity $x_e(t)$. We refer to x_e/c_e as the conductivity of e and to $r_e = c_e/x_e$ as the resistance of e . For a solution f of $Af = b_i$, we use

$$E_x(f) = \begin{cases} \sum_e r_e f_e^2 & \text{if } \text{supp } f \subseteq \text{supp } x, \\ \infty & \text{if } \text{supp } f \not\subseteq \text{supp } x. \end{cases}$$

¹Since Steiner trees are well approximated by Minimum Spanning Trees (MST), there are compact linear programs for the MST problem, and the Physarum dynamics can solve LPs, in a sense, we know already that the Physarum dynamics can be used to construct a good network. We are searching for a model that doesn't go through such an "unnatural" reductions and whose only variables are those representing the flows on the edges.

²The reader may want to think of A as the node-arc incidence matrix of a connected undirected graph G with n nodes and m edges, i.e., for each $e = (u, v) \in E$, the column A_e has an entry $+1$ in position u and entry -1 in position v ; the orientation of the edge is arbitrary, but fixed. We have k different source-sink pairs $(s_i^{(1)}, s_i^{(2)})$, $1 \leq i \leq k$. Let $b_i \in \mathbb{R}^n$ be the vector with entry $+1$ in position $s_i^{(1)}$ and entry -1 in position $s_i^{(2)}$. All other entries of b_i are zero. Since G is assumed to be connected, the linear system $Af = b_i$ has a solution for all i .

to denote the energy of f with respect to x . Let $q_i(x) \in \mathbb{R}^m$ or simply q_i be the minimum energy solution³ of $Af = b_i$ with respect to x . The minimum energy solution (see Section 3 for details) is induced by node potentials $p_i \in \mathbb{R}^n$ with components p_{vi} such that for each edge $e = (u, v)$, $q_{ei} = \frac{x_e}{c_e}(p_{vi} - p_{ui}) = x_e A_e^T p_i / c_e$ or more compactly $q_i = XC^{-1}A^T p_i$, where X and C are diagonal matrices in $\mathbb{R}^{m \times m}$ with entries x_e and c_e , respectively. The node potentials satisfy the equations $AXC^{-1}A^T p_i = b_i$. We use $L(x)$ to denote the matrix $AXC^{-1}A^T$. Let $\Lambda_{ei} = A_e^T p_i / c_e$. Then $q_{ei} = x_e \Lambda_{ei}$. We summarize the notation:

$$\begin{aligned}
c &\in \mathbb{R}^m, \text{ vector of edge costs, } c > 0, C = \text{diag}(x), \\
x &\in \mathbb{R}^m, \text{ vector of edge capacities, } x \geq 0, X = \text{diag}(x), \\
A &\in \mathbb{R}^{n \times m}, \text{ constraint matrix, elements } A_{ve}, \\
u, v, w &\in [n], \\
e, e' &\in [m], \\
A_e &= e\text{-th column of } A, \\
i, j &\in [k], \\
B &\in \mathbb{R}^{n \times k}, \text{ matrix of right hand sides, elements } B_{vi}, \\
B_i \text{ or } b_i &= i\text{-th column of } B, \\
L(x) &= AXC^{-1}A^T, \text{ Laplacian matrix,} \\
Q &\in \mathbb{R}^{m \times k}, \text{ matrix of electrical flows, elements } Q_{ei}, AQ = B, \\
q_i \text{ or } Q_i &= i\text{-th column of } Q, \\
Q_e &= e\text{-th row of } Q, \\
P &\in \mathbb{R}^{n \times k}, \text{ matrix of node potentials, elements } P_{vi}, L(x)P = B, \\
p_i \text{ or } P_i &= i\text{-th column of } P, \\
P_v &= v\text{-th row of } P, \\
\Lambda &\in \mathbb{R}^{m \times k}, \text{ matrix of normalized potential drops, elements } \Lambda_{ei}, \Lambda_{ei} = A_e^T p_i / c_e, \\
\Lambda_e &= e\text{-th row of } \Lambda
\end{aligned}$$

The trace of a matrix is the sum of its diagonal elements. Thus $\text{Tr}(B^T P) = \sum_i b_i^T p_i$. In the case of Q and P it will always be clear from the index (i or e in the case of Q and v or i in the case of P), where we refer to a row or column.

In the multi-commodity flow setting, we have many right hand sides and the solution q_i realizes the i -th demand b_i . We let the vector Q_e of values Q_{ei} for any edge e determine the capacity of an edge and study different ways of combining the individual solutions, in particular, one-norm and

³Continuation of Footnote 2: We view the graph as an electrical network where edge e has resistance $r_e = c_e/x_e$. Let $q_i \in \mathbb{R}^m$ with components q_{ei} be the electrical flow realizing the demand b_i , i.e., $Aq_i = b_i$. It is well known that the electrical flow is the minimum energy solution to $Af_i = b_i$ and that electrical flows are induced by node potentials $p_i \in \mathbb{R}^n$ with components p_{vi} such that for each edge $e = (u, v)$, $q_{ei} = \frac{x_e}{c_e}(p_{vi} - p_{ui}) = x_e A_e^T p_i / c_e$. $\Lambda_{ei} = A_e^T p_i / c_e = (p_{vi} - p_{ui})/c_e$ is the normalized potential drop across the edge e ; normalized = potential drop per unit of length.

two-norm⁴. This leads to the following dynamics:

$$\dot{x}_e = -x_e + \sum_i |q_{ei}| = x_e \left(-1 + \sum_i \frac{|q_{ei}|}{x_e} \right) = x_e \left(-1 + \sum_i |\Lambda_{ei}| \right) = x_e (\|\Lambda_e\|_1 - 1), \quad (1)$$

$$\dot{x}_e = -x_e + \sqrt{\sum_i q_{ei}^2} = x_e \left(\sqrt{\sum_i \left(\frac{q_{ei}}{x_e} \right)^2} - 1 \right) = x_e \left(\sqrt{\sum_i \Lambda_{ei}^2} - 1 \right) = x_e (\|\Lambda_e\|_2 - 1). \quad (2)$$

In (1), we form the one-norm $\|\Lambda_e\|_1$ of the different normalized potential drops across any edge e , and in (2), we form the two-norm $\|\Lambda_e\|_2$, and in (2). For $k = 1$, the one-norm and the two-norm dynamics coincide. The results of this paper suggest that the two-norm dynamics is the appropriate generalization to larger k .

The following *generalized Physarum dynamics* introduced in [Bon16] subsumes the two-norm dynamics as a special case. For each $e \in E$, let g_e be a non-negative, increasing and differentiable function with $g_e(1) = 1$:

$$\dot{x}_e = x_e (g_e (\|\Lambda_e\|_2) - 1). \quad (3)$$

The two-norm dynamics is a special case with $g_e(z) = 1 + (z - 1)$. Other examples are $g_e(z) = 1 + d_e(z - 1)$ and $g_e(z) = 1 + d_e(z^2 - 1)$ where $d_e > 0$ is the “reactivity” [KKM20] of edge e , $g_e(z) = z^{\mu_e}$ for some $\mu_e > 0$ or $g_e(z) = (1 + \alpha_e)z^{\mu_e} / (1 + \alpha_e z^{\mu_e})$ for some $\mu_e, \alpha_e > 0$.

The right hand sides of (1) to (3) are defined for any

$$x \in \Omega = \left\{ x \in \mathbb{R}_{\geq 0}^m : \text{for all } i \text{ there is a solution } f_i \text{ to } Af = b_i \text{ with } \text{supp } f_i \subseteq \text{supp } x \right\}.$$

In the analytical part of the paper, we ask and answer the following questions for the generalized Physarum dynamics. We have little to say about the one-norm dynamics.

- Does the dynamics have a solution $x(t)$ with $t \in [0, \infty)$?
- Does the dynamics converge?
- What are the fixed points and the limit points of the dynamics?
- What does the dynamics optimize?
- How can we characterize the limit points?

In the experimental part of the paper, we perform computer and pencil-and-paper simulations of the dynamics and address the following questions:

- How strong are the sharing effects of the dynamics? How far deviate individual flows from their shortest realization in order to benefit from sharing edges with other flows?
- Does the dynamics generate “nice” networks?

Existence: Solutions with domain $[0, \infty)$ exist for the generalized Physarum dynamics.

Theorem 1. *Let $x(0) \in \mathbb{R}_{>0}^m$. The generalized Physarum dynamics has a solution $t \mapsto x(t) \in \mathbb{R}_{>0}^m$ for $t \in [0, \infty)$.*

⁴Continuation of Footnote 2: In the setting of Footnote 2, the q_i ’s are flows in the network G . The fact that flows from different demand pairs on the same edge do not cancel each other (not even partially) seems a bit strange at the microscopic level. After all, physically, only the cytoplasm is being transported. How does an edge “distinguish” between the cytoplasm of pair i and the cytoplasm of pair i' ? When $k=1$, clearly this was not an issue.

However, the flow of cytoplasm is in reality a shuttle-flow, going back and forth between source and sink, and changing directions with some frequency. Aggregating flow using norms makes sense if we assume that the source-sink oscillations happen with uncorrelated frequencies. In that case, the power of two linearly combined signals is indeed the sum of the powers of the two signals, since the power of $A+B$ is the power of A plus the power of B plus twice the covariance of A and B (which is zero for uncorrelated A and B).

Cost and Energy Dissipation of a Capacity Vector: The cost of a capacity vector x is defined as

$$\mathcal{C}(x) = c^T x = \sum_e c_e x_e.$$

The energy dissipation for a single demand b induced by a capacity vector x is defined as

$$\min_{f; Af=b} E_x(f) = \sum_e r_e q_e^2 = b^T p = p^T L(x)p,$$

where q is the minimum energy solution of $Af = b$ with respect to x and p is the corresponding node potential. We will show the second equality in Section 3. The last equality follows from $L(x)p = b$. The energy dissipation $\mathcal{E}(x)$ for a set of k demands b_1, \dots, b_k is the sum of the energy dissipations for the individual demands, i.e.,

$$\mathcal{E}(x) = \sum_i b_i^T p_i = P^T L(x)P,$$

where p_i is the node potential with respect to the minimum energy solution q_i to the i -th demand.

Fixed Points: The fixed points of a dynamics are the points x with $\dot{x}_e = 0$ for all e . We use \mathcal{F}_1 and \mathcal{F}_g to denote the fixed points (also called equilibrium points) of the one-norm and the generalized dynamics.

Lemma 1 (The fixed points of the one-norm dynamics). $x \in \mathcal{F}_1$ iff for all e either $x_e = 0$ or $\|\Lambda_e\|_1 = 1$. The latter condition is equivalent to $\|Q_e\|_1 = x_e$ and equivalent to $\|\Lambda_e\|_1 = c_e$.

Lemma 2 (The fixed points of the generalized Physarum dynamics). $x \in \mathcal{F}_g$ iff for all e either $x_e = 0$ or $\|\Lambda_e\|_2 = 1$. The latter condition can be expressed equivalently by $\|A_e^T P\|_2 = c_e$ and also by $x_e = \|Q_e\|_2$. Further, for every $x \in \mathcal{F}_g$ we have $x \geq 0$, $AQ = B$, and

$$\text{Tr}(B^T P) = \mathcal{E}(x) = \mathcal{C}(x) = c^T x,$$

i.e., for fixed points of the generalized Physarum dynamics the cost equals the energy dissipation.

Convergence: Let

$$\mathcal{L}(x) = \frac{1}{2}(\mathcal{C}(x) + \mathcal{E}(x)) = \frac{1}{2}(c^T x + \sum_i b_i^T p_i).$$

We show in Section 6 that the function \mathcal{L} is a Lyapunov function for the generalized Physarum dynamics, i.e., $\frac{d}{dt}\mathcal{L}(x(t)) = \langle \nabla \mathcal{L}, \dot{x} \rangle \leq 0$ for all t and $\langle \nabla \mathcal{L}, \dot{x} \rangle = 0$ if and only if $x \in \mathcal{F}_g$. In the case $k = 1$, \mathcal{L} is also a Lyapunov function for the one-norm dynamics as shown in [KKM20]. Let

$$\mathcal{V} = \{x : \langle \nabla \mathcal{L}, \dot{x} \rangle = 0\}.$$

What do the Dynamics Optimize? We do not know for the one-norm dynamics. The generalized Physarum dynamics minimizes \mathcal{L} .

Theorem 2. $\mathcal{F}_g = \mathcal{V}$ and the generalized Physarum dynamics converges to \mathcal{V} . Moreover, if the set \mathcal{F}_g is finite and any two points in \mathcal{F}_g have distinct values of \mathcal{L} , the dynamics $x(t)$ converges to $x^* = \text{argmin}_{x \in \mathbb{R}_{\geq 0}^m} \mathcal{L}(x)$.

Further Properties of the Lyapunov Minimum: The minimum of the Lyapunov function can also be characterized in alternative ways.

Theorem 3. The following quantities $\text{Min}Q$, $\text{Max}P$, and $\text{Min}L$ are equal.

$$\text{Min}Q = \min_{Q \in \mathbb{R}^{m \times k}} \left\{ \sum_e c_e \|Q_e\|_2 : AQ = B \right\}, \quad (4)$$

$$\text{Max}P = \max_{P \in \mathbb{R}^{n \times k}} \left\{ \text{Tr}(B^T P) : \|A_e^T P\|_2 \leq c_e \text{ for all } e \right\}, \quad (5)$$

$$\text{Min}L = \min_{x \in \mathbb{R}_{\geq 0}^m} \mathcal{L}(x). \quad (6)$$

Moreover, there are optimizers Q^* , R^* and x^* such that

$$\begin{aligned} x_e^* &= \|Q_e^*\|_2 \quad \text{for all } e, \\ L(x^*)P^* &= B, \\ Q^* &= X^*C^{-1}A^TP^*. \end{aligned}$$

Case Studies: We performed three case studies, two small and the third inspired by the wet-lab experiment by [TKN07]. The first example (Section 2.1) can be treated analytically, we consider a ring with three nodes with a demand of one between any pair of nodes. We will see that a solution using all three edges is superior to a solution using only two edges. Also, we see confirmed that for fixed points of the two-norm dynamics the cost of the network and the total energy dissipation is the same. The second example (Section 2.2) concerns flow in the Bow-Tie graph shown in Figure 3. We will investigate the incentive for sharing links. In this example, the demands can share a link at the cost of increasing the distance between the terminals. We will see that sharing pays off provided that the detour is not too big. The third example 2.3 is based on the example in [TKN07]. We will see that the dynamics forms nice networks.

Organization of the Paper: In Section 2, we report about paper-and-pencil and computer experiments. The analytical part starts with Section 3. We review basic facts about electrical flows. In subsequent sections, we prove the existence of a solution defined for $t \in [0, \infty)$, characterize the fixed points, prove that \mathcal{L} is Lyapunov function, derive further properties of the Lyapunov minimum, show convergence to the Lyapunov minimum, and finally make a connection to mirror descent.

2 Case Studies

2.1 Multi-commodity Flow in a Ring

Consider a graph consisting of three vertices a , b , and c and three edges connecting them into a 3-cycle. All edges have cost one and we have a demand of one between any pair of nodes. An equilibrium uses either two edges or three edges.

2.1.1 Two Edge Solution

We will see below that, for each of the dynamics, the solution is symmetric, i.e., both edges have the same capacity in equilibrium, say z . The flow across both edges is two. For each demand, the potential drop on each edge is $1/z$. So the total energy spent is $\mathcal{E} = 2/z + 2 \cdot 1/z = 4/z$ and the total cost $\mathcal{C} = 2z$. Thus $\mathcal{C} + \mathcal{E} = 4/z + 2z$.

One-Norm Dynamics: The current across each edge is 2 and hence $z = 2$ for each of the existing edges. Thus $\mathcal{C} = c^T z = 4$, $\mathcal{E} = \sum_i b_i^T p_i = 4/z = 2$, and $\mathcal{C} + \mathcal{E} = 6$.

Two-Norm Dynamics The current across each edge is $1 + 1$ and hence $z = \sqrt{2}$. Thus $\mathcal{C} = c^T z = 2\sqrt{2}$, $\mathcal{E} = \sum_i b_i^T p_i = 4/\sqrt{2} = 2\sqrt{2}$ and $\mathcal{C} + \mathcal{E} = 4\sqrt{2}$. Note that $\mathcal{C} = 2\sqrt{2} = \mathcal{E}$. This is not a coincidence as we show in Lemma 7.

Optimum: We have $\mathcal{C} + \mathcal{E} = 4/z + 2z$. The optimum is attained for $z = \sqrt{2}$. Note that this corresponds to the equilibrium of the two-norm. This is not a coincidence as we show in Theorem 4.

2.1.2 Three Edge Solution

We will see below that, for each of the dynamics, the solution is symmetric, i.e., all edges have the same capacity in equilibrium, say z , and hence the same resistance $1/z$. Then $\mathcal{C} = 3z$. Each demand is routed partly the short way and partly the long way. Since the long way has twice the resistance, the amount routed the short way is twice the amount routed the long way, i.e., $2/3$ of each demand is routed the short way and $1/3$ is routed the long way.

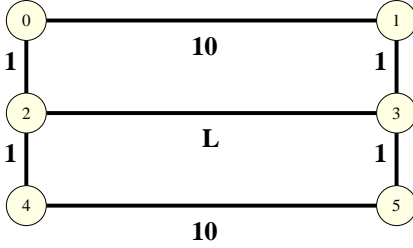


Figure 2: The top and the bottom horizontal edge have cost 10, the middle horizontal edge has cost L , and all other edges have cost 1. We are sending one unit between nodes 0 and 1 and one unit between nodes 4 and 5.

For each demand, let Δ be the potential drop between source and sink. The total energy spent is 3Δ . The potential drop Δ must be such that it can drive a current of $2/3$ across a wire of conductance z . Thus $\Delta = 2/(3z)$. We obtain $\mathcal{C} + \mathcal{E} = 3z + 2/z$.

One-Norm Dynamics: z is equal to the total current flowing across an edge and hence $z = 2/3 + 2 \cdot 1/3 = 4/3$ and $\Delta = 1/2$. So $\mathcal{C} = c^T z = 4$, $\mathcal{E} = \sum_i b_i p_i = 3/2$, and $\mathcal{C} + \mathcal{E} = 11/2$. This is better than for the two-edge equilibrium.

Two-Norm Dynamics For each edge, we have one flow of value $2/3$ and two flows of value $1/3$ and hence $z^2 = 4/9 + 2 \cdot 1/9 = 6/9$. Thus $z = \sqrt{2/3}$. Δ must be such that it can drive a current of $2/3$ across a wire of conductance $\sqrt{2/3}$ and hence $\Delta = \sqrt{2/3}$.

Hence $\mathcal{C} = c^T z = 3 \cdot \sqrt{2/3} = \sqrt{6}$ and $\mathcal{E} = \sum_i b_i p_i = 3 \cdot \sqrt{2/3} = \sqrt{6}$. Note that again we have the same value for the cost \mathcal{C} and the total energy spent \mathcal{E} . For the sum, we obtain $\mathcal{C} + \mathcal{E} = 2\sqrt{6}$. This is better than the two-edge equilibrium.

Optimum: For a general value of z , we have $\mathcal{C} + \mathcal{E} = 3z + 2/z$. This is minimized for $z = \sqrt{2/3}$, i.e., the equilibrium of the two-norm is equal to the minimum combined cost solution.

2.1.3 Computer Simulations

Table 1 shows the results of a typical simulation. For the simulation we discretized the differential equation and applied an Euler forward scheme.

	the final z -values of the three edges		
two-norm dynamics	0.8160	0.8167	0.8166
one-norm dynamics	1.331	1.327	1.342

Table 1: The initial z -values were chosen randomly between $1/1000$ and 1. In all cases, the system converged to the 3-edge equilibrium. Note that $0.82 \approx \sqrt{2/3}$ and $1.33 \approx 4/3$.

2.2 The Bow-Tie Graph

Consider the graph shown in Figure 2; we refer to this graph as a bow-tie. The edge costs are as shown and we are sending one unit each between nodes 0 and 1 and nodes 4 and 5, i.e., $b_0 = (1, -1, 0, 0, 0, 0)$ and $b_1 = (0, 0, 0, 0, 1, -1)$. For each pair the direct path connecting the pair has length 10, the path using the middle edge has length $L + 2$ and the path using the edge connecting the other pair has length 14. Figures 3 and 4 show the results of a simulation. Initial x -values were chosen randomly in the interval $[1, 10]$. We observe:

- For $L \leq 8$, both dynamics generate essentially the same solution. All flow is essentially routed through the middle edge.

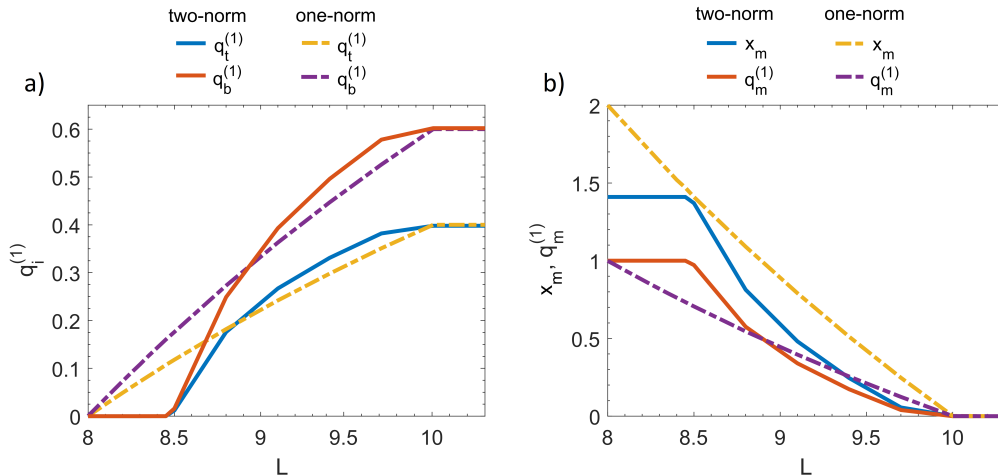


Figure 3: Simulation of the Bow-Tie Graph: The plot depicts the quantities $q_b^{(1)}$, $q_m^{(1)}$, and $q_t^{(1)}$ (= the split-up of the flow from node 0 to node 1 across the three horizontal edges bottom, middle, and top) and x_m (= the capacity of the middle edge) as a function of L in the range $[8, 10.3]$. For $L < 8$, the quantities are as for $L = 8$ and for $L > 10.3$, the quantities are as for $L = 10.3$. For $q^{(2)}$ the flow across the middle edge is the same and the flow across the other edges is reversed. For all L , $q_b^{(1)} + q_m^{(1)} + q_t^{(1)} = 1$. (1) The image on the left shows $q_b^{(1)}$ and $q_t^{(1)}$. (2) The image on the right shows the capacity x_m and the flow $q_m^{(1)}$ across the middle edge. We have $x_m = \sqrt{2(q_m^{(1)})^2} = \sqrt{2} \cdot q_m^{(1)}$ in the case of the two-norm and $x_m = 2q_m^{(1)}$ in the case of the one-norm.

L	6.5	6.8	7.1	7.4	7.7	8.0	8.3	8.6	8.9	9.2	9.5	9.8
\mathcal{C}	13.2	13.6	14.0	14.5	14.9	15.3	15.7	16.1	16.4	16.6	16.7	16.7
\mathcal{E}	13.2	13.6	14.0	14.5	14.9	15.3	15.7	16.1	16.4	16.6	16.7	16.7

Figure 4: . Simulation results for the two-norm dynamics for the bow-tie graph. The cost $\mathcal{C} = c^T x$ and the energy $\mathcal{E} = \sum_i b_i^T p_i$ for the limit states for different values of L . Note that $\mathcal{C} = \mathcal{E}$ always.

- For the two-norm dynamics: For $L < 8.5$, the sharing effect is strong and basically all flow is routed through the middle edge. Starting at $L = 8.5$, the top and the bottom edge are also used. For $L \geq 10$, only the top and the bottom edge are used.
- For the one-norm dynamics: Starting at $L = 8.05$, the top and the bottom edge are also used. For $L \geq 10.3$, only the top and the bottom edge are used.
- For the two-norm dynamics, the cost \mathcal{C} and the dissipated energy \mathcal{E} are equal in the limit; see Figure 4.

2.3 A Case Study Inspired by [TTS⁺10]

In [TTS⁺10] the slime molds ability to construct elegant networks is investigated. The slime is allowed to grow in a region that is shaped according to the greater Tokyo region and food is provided at many different places. Figure 1 shows the results of the wet-lab experiment and compares a network constructed by the slime to the railroad network around Tokyo. The paper also reports about a computer experiment. Repeatedly a pair of food sources was chosen at random and a step of the shortest path dynamics was executed. Figure 4 in [TTS⁺10] shows the results

of the computer experiment. No details are given in the paper and also the positions of the food sources are not given in detail.

We tried to repeat the experiment with the two-norm dynamics. For this purpose, we digitized the boundary of the Greater Tokyo region in the form of a polygonal region and overlaid a regular grid in which each node is connected to its up to eight neighbors (north, northwest, west, southwest, south, southeast, east, northeast) inside the region. The edge lengths are 1 for the horizontal and vertical edges and 1.41 for the diagonal edges. We perturbed the edge lengths slightly by adding $r \cdot 0.05$ for a random integer $r \in [-3, 3]$ so as to avoid many equal length path. We chose the terminals in two different ways.

First choice: We chose the largest 25 cities Greater Tokyo region according to Wikipedia and generated 140 demands. Each city was connected to all other cities whose distance is below a certain threshold. For the threshold we chose about 1/2 times the diameter of the region. The left side of Figure 5 shows the input and Figure 6 shows the output of a computer simulation.

Second choice: We mimicked the choice of sites used in [TTS⁺10]. We generated 282 demands again between any pair of sites whose distance is below a certain threshold. The demands are 1, except if one of the terminals corresponds to Tokyo. Then the demand is seven; this is as in [TTS⁺10]. The right side of Figure 5 shows the input and Figure 7 shows the output of a computer simulation.

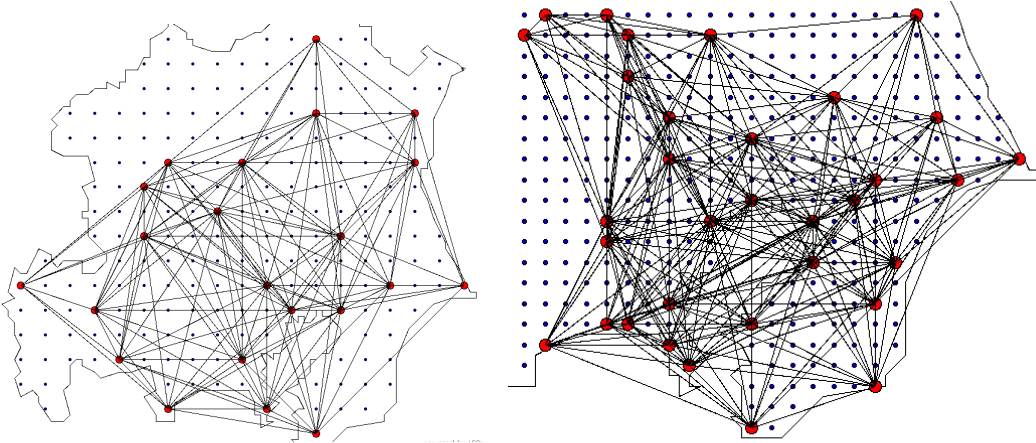


Figure 5: The polygonal region on the left is a digitization of the Greater Tokyo Region. The red dots indicate major cities. We set up 140 demands. For each red city, we created a demand of one unit to any other red city within a certain distance threshold. The threshold is about 1/2 the distance between the topmost and the bottommost red point. The region on the right is approximately the right lower quadrant of the region on the left. For the placement of the terminals we tried to copy the placement shown in Figure 1. We set up 282 demands, again between cities below a certain distance threshold. The demands are one, except if one of the terminals corresponds to Tokyo. Then the demand is seven; this is as in [TTS⁺10].

3 Preliminaries

We recall the definition of energy dissipation and cost. For a capacity vector $x \in \mathbb{R}_{\geq 0}^m$ and a vector $f \in \mathbb{R}^m$ with $\text{supp}(f) \subseteq \text{supp}(x)$, we use

$$E_x(f) = \begin{cases} \sum_e (c_e/x_e) f_e^2 & \text{if } \text{supp } f \subseteq \text{supp } x, \\ \infty & \text{if } \text{supp } f \not\subseteq \text{supp } x. \end{cases}$$

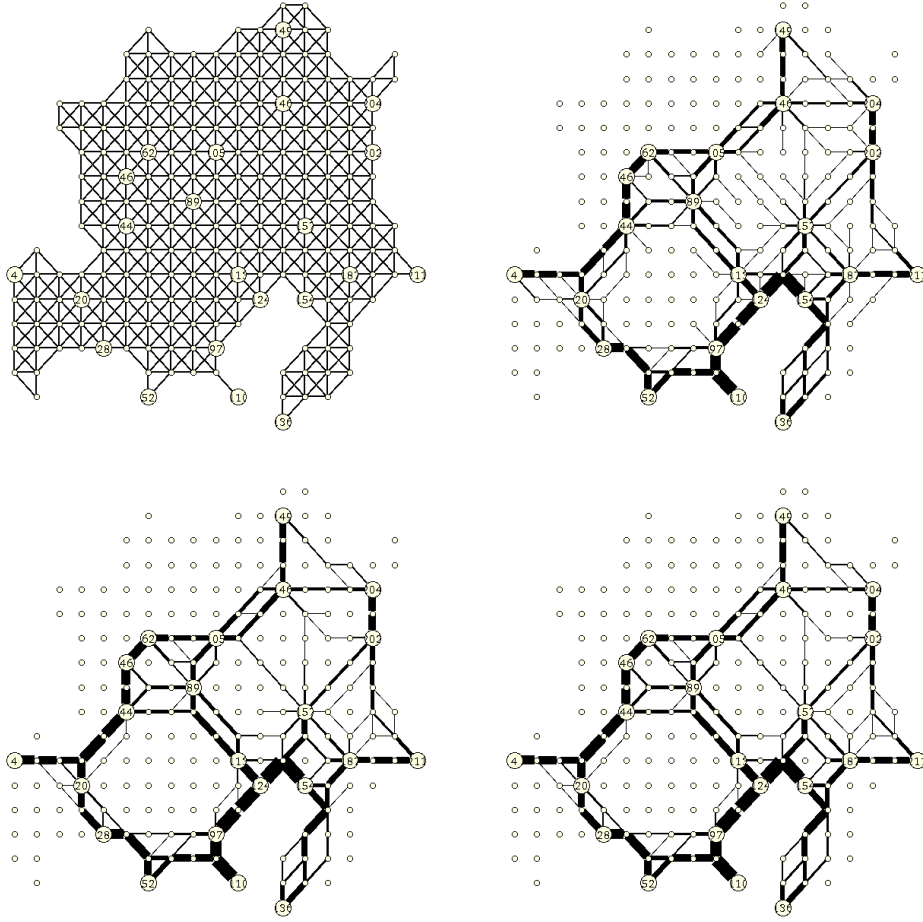


Figure 6: An output of a simulation of the two-norm dynamics on the left instance in Figure 5. The graph in the upper left corner shows the initial graph. Each node is connected to its up to 8 neighbors. The length of the horizontal and vertical edges is approximately 1, the length of the diagonals is approximately 1.41. All capacities are 0.5 initially and the capacity of an edge is indicated by its thickness. The following figures show the state after 1950 and 4875 iterations. For the situation after 4875 iterations, we also show the reduced graph where we iteratively removed nodes of degree one (which are not terminals). The numbers inside the nodes are unique identifiers; they have no meaning beyond this.

to denote the *energy dissipation* of f with respect to x . Strictly speaking we should sum only over the e in $\text{supp } x$. We use the convention $0^2/0 = 0$ to justify summing over all edges e . Further, we use

$$\mathcal{C}(f) = \sum_e c_e |f_e| = c^T |f|$$

to denote the *cost* of f . Note that

$$E_x(x) = \sum_e (c_e/x_e) x_e^2 = \sum_e c_e x_e = \mathcal{C}(x).$$

We use R to denote the diagonal matrix with entries c_e/x_e . Energy-minimizing solutions are

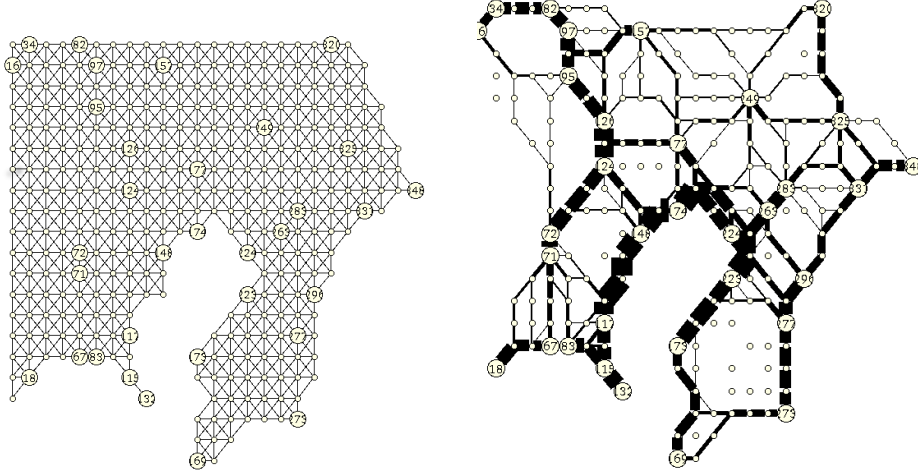


Figure 7: An output of a simulation of the two-norm dynamics on the right instance in Figure 5. The graph in the upper left corner shows the initial graph. Each node is connected to its up to 8 neighbors. The length of the horizontal and vertical edges is approximately 1, the length of the diagonals is approximately 1.41. All capacities are 0.5 initially and the capacity of an edge is indicated by its thickness. The figure on the right show the state after 16000 iterations where we iteratively removed nodes of degree one.

induced by node potentials $p \in \mathbb{R}^n$ according to the following equations:

$$b = Aq, \quad (7)$$

$$q = R^{-1}A^T p, \quad (8)$$

$$AR^{-1}A^T p = b. \quad (9)$$

We give a short justification why the equations above characterize the energy minimizing solution to the linear system. The energy minimizing solution q minimizes the quadratic function $\sum_e (c_e/x_e)q_e^2$ subject to the constraints $Aq = b$ and $\text{supp}(q) \subseteq \text{supp}(x)$. The KKT conditions (see [BV04, Subsection 5.5]) state that at the optimum, the gradient of the objective is a linear combination of the gradients of the constraints, i.e.,

$$2(c_e/x_e)q_e = \sum_i p_i A_{i,e} \quad \text{for all } e \in \text{supp}(x)$$

for some vector $p \in \mathbb{R}^n$ and $q_e = 0$ for $e \notin \text{supp}(x)$. Absorbing the factor 2 into p yields equation (8). Substitution of (8) into (7) gives (9). The energy-minimizing solution is unique. It exists if and only if $b \in \text{Im}A$. Node potentials p are not unique, but the values of $b^T p$ and $p^T L(x)p$ do not depend on the node potential.

Lemma 3. *Assume $x > 0$. Then $\text{Ker}L(x) = \text{Ker}A^T$ and $\text{Im}L(x) = \text{Im}A$. The values $b^T p$, $b^T L(x)p$ and $q = XC^{-1}A^T p$ do not depend on the particular solution of $L(x)p = b$.*

Proof. Clearly, $\text{Ker}A^T \subseteq \text{Ker}L(x)$. So assume $z \in \text{Ker}L(x)$. Then $L(x)z = 0$ and hence $z^T L(x)z = 0$. Let $D^{1/2}$ be the diagonal matrix with entries $\sqrt{x_e/c_e}$. Then

$$0 = z^T L(x)z = z^T AD^{1/2}D^{1/2}A^T z = \|D^{1/2}A^T z\|_2^2$$

and hence $D^{1/2}A^T z = 0$ and further $0 = A^T z$. So $z \in \text{Ker}A^T$.

Clearly, $\text{Im}L(x) \subseteq \text{Im}A$. So assume $b \notin \text{Im}L(x)$. Then the rank of the matrix obtained by augmenting $L(x)$ by the column b is larger than the rank of $L(x)$ (Rouché-Capelli theorem) and

hence there is a vector r such that $r^T b \neq 0$ and $r^T L(x) = 0$. Since $L(x)$ is symmetric, $L(x)r = 0$ and hence $r \in \text{Ker}L(x) = \text{Ker}A^T$. So $0 = A^T r = (r^T A)^T$. Thus r also proves $b \notin \text{Im}A$.

Let p and \bar{p} be node potentials. Then $L(x)p = b = L(x)\bar{p}$ and hence $\bar{p} - p \in \text{Ker}L(x)$. Then

$$b^T \bar{p} = b^T p + b^T (\bar{p} - p) = b^T p + p^T L(x)^T (\bar{p} - p) = b^T p + p^T L(x) (\bar{p} - p) = b^T p$$

and

$$XC^{-1}A^T \bar{p} = XC^{-1}A^T p + XC^{-1}A^T (\bar{p} - p) = XC^{-1}A^T p.$$

Finally, $b^T p = p^T L(x)p$. □

For the arc-node incidence matrix A of a connected graph, the kernel $\text{Ker}A^T$ consists of the all-ones vector in \mathbb{R}^n . We can make the node potential unique by requiring $p_v = 0$ for some fixed node v , i.e., by grounding node v .

Lemma 4. *Let ℓ be the dimension of $\text{Ker}A^T$ and let $K \in \mathbb{R}^{n \times \ell}$ be a matrix whose columns form a basis of $\text{Ker}A^T$. Let $V' \subseteq [n]$ with $|V'| = \ell$ be such that the submatrix of K with rows selected by V' is nonsingular. Then the solution p to $L(x)p = b$ with $p_v = 0$ for all $v \in V'$ is unique, i.e. “grounding all nodes in V' makes the potential unique”.*

Proof. Observe first that such a solution exists. Let p be an arbitrary solution to $L(x)p = b$. Then there is a vector $\lambda \in \mathbb{R}^\ell$ such that $(K\lambda)_v = p_v$ for all $v \in V'$ and hence $p - K\lambda$ is the desired node potential. Assume now that we have two solutions p and p' with $p_v = p'_v$ for all $v \in V'$. Then $p - p' \in \text{Ker}L(x) = \text{Ker}A^T$ and $(p - p')_v = 0$ for all $v \in V'$. Since $p - p' \in \text{Ker}A^T$ there is a $\lambda \in \mathbb{R}^\ell$ such that $p - p' = K\lambda$. Then $(K\lambda)_v = 0$ for all $v \in V'$. Since the columns of K are independent, this implies $\lambda = 0$ and hence $p = p'$. □

The next Lemma gives alternative expressions for the energy $E_x(q)$ of the minimum energy solution.

Lemma 5. $E_x(q) = \sum_e (c_e/x_e) q_e^2 = b^T p = p^T L(x)p$, where p is any solution of (9).

Proof. This holds since

$$E_x(q) = q^T Rq = p^T AR^{-1}RR^{-1}A^T p = p^T AR^{-1}A^T p = p^T L(x)p = p^T b.$$
□

Finally, we recapitulate a bound on the components of q established in [SV16b] and slightly improved form in [BBK⁺19, Lemma 3.3].

Lemma 6. *Let D be the maximum absolute value of a square submatrix of A . Then $|q_e| \leq D\|b\|_1$ for every $e \in [m]$.*

4 Existence of a Solution

We prove Theorem 1. The right-hand side (3) is locally Lipschitz-continuous in x . The function g_e is locally Lipschitz by assumption, the q_i 's are infinitely often differentiable rational functions in the x_e and hence locally Lipschitz. Furthermore, locally Lipschitz-continuous functions are closed under additions and multiplications. Thus $x(t)$ is defined and unique for $t \in [0, t_0)$ for some t_0 .

Since g_e is non-negative, we have $\dot{x}_e \geq -x$ and thus $x_e \geq x_e(0)e^{-t}$. Hence, $x(t) > 0$ for all t . By assumption $b_i \in \text{Im}A$ for all i , and hence whenever $x(t) > 0$, we have solutions q_i with $\text{supp}(q_i) \subseteq \text{supp}(x)$.

In Section 6, we will show that \mathcal{L} is a Lyapunov function for the dynamics (3). Thus

$$c^T x \leq \mathcal{L}(x) \leq \mathcal{L}(x(0))$$

and hence x stays in a bounded domain.

It now follows from general results about the solutions of ordinary differential equations [Har02, Corollary 3.2] that $t_0 = \infty$.

5 Fixed Points

A point x is a fixed point iff $\dot{x} = 0$. We use \mathcal{F}_g for the set of fixed points of (3).

Lemma 7 (The fixed points of the generalized Physarum dynamics). *$x \in \mathcal{F}_g$ iff for all e either $x_e = 0$ or $\|\Lambda_e\|_2 = 1$. The latter condition is equivalent to $x_e = \|Q_e\|_2$ or $\|A_e^T P\|_2 = c_e$. For $x \in \mathcal{F}_g$, $\mathcal{C}(x) = \mathcal{E}(x)$.*

Proof. We have $\dot{x} = 0$ iff we have $x_e = 0$ or $g_e(\|\Lambda_e\|_2) = 1$ for all e . Since g_e is increasing and $g_e(1) = 1$, the latter condition is tantamount to $\|\Lambda_e\|_2 = 1$ which expands to $\sum_i (A_e^T p_i)^2 = c_e^2$. Multiplying both sides by $(x_e/c_e)^2$ yields $x_e^2 = \sum_i q_{ei}^2$.

For $x \in \mathcal{F}_g$, we have

$$\mathcal{E}(x) = \sum_e \sum_i \frac{c_e}{x_e} q_{ei}^2 = \sum_e \frac{c_e}{x_e} \cdot x_e^2 = \sum_e c_e x_e = \mathcal{C}(x).$$

□

6 Lyapunov Function

Let

$$\mathcal{L}(x) = \frac{1}{2} \left(c^T x + \sum_{i=1}^k b_i^T p_i \right).$$

We will show that \mathcal{L} is a Lyapunov function for the dynamics (3). The function \mathcal{L} was introduced in [FDCP18]. For $k = 1$, [FCP18] shows that \mathcal{L} is a Lyapunov function for the one-norm dynamics and [KKM20] shows that this holds true also for the generalized Physarum dynamics. The calculations below generalize the calculations in these papers. They are similar to the calculations in [Bon19, Lemma 2.6].

Lemma 8 (Gradient of \mathcal{L}). *For all $e \in E$,*

$$\frac{\partial}{\partial x_e} \mathcal{L}(x) = \frac{c_e}{2} (1 - \|\Lambda_e\|_2^2). \quad (10)$$

Proof. Recall $L(x) = AXC^{-1}A^T$. Let $e \in [m]$ be arbitrary. Then $\frac{\partial}{\partial x_e} L(x) = \frac{1}{c_e} A_e A_e^T$. From $L(x)p = b$ and $\frac{\partial}{\partial x_e} b = 0$, we obtain

$$0 = \frac{\partial}{\partial x_e} L(x)p = \frac{\partial L(x)}{\partial x_e} p + L(x) \frac{\partial p}{\partial x_e}$$

and thus

$$L(x) \frac{\partial p}{\partial x_e} = -\frac{1}{c_e} A_e A_e^T p.$$

Hence, we have

$$\frac{\partial}{\partial x_e} b^T p = b^T \frac{\partial p}{\partial x_e} = p^T L(x) \frac{\partial p}{\partial x_e} = -\frac{1}{c_e} p^T A_e A_e^T p = -c_e \left(\frac{A_e^T p}{c_e} \right)^2,$$

and more generally,

$$\frac{\partial}{\partial x_e} \sum_i b_i^T p_i = -c_e \sum_i \left(\frac{A_e^T p_i}{c_e} \right)^2 = -c_e \|\Lambda_e\|_2^2.$$

The claim follows. □

Theorem 4. *The function $\mathcal{L} : \Omega \mapsto \mathbb{R}$ is a Lyapunov function for the dynamics (3), i.e., $\frac{d}{dt}\mathcal{L}(x(t)) \leq 0$ for all t . Let*

$$\mathcal{V} = \{x \in \Omega : \langle \nabla \mathcal{L}(x), \dot{x} \rangle\}.$$

Then $\mathcal{V} = \mathcal{F}_g$.

Proof. Since $\frac{d}{dt}\mathcal{L}(x(t)) = \langle \nabla \mathcal{L}(x), \dot{x} \rangle$, we obtain

$$\frac{d}{dt}\mathcal{L}(x(t)) = \sum_e \frac{c_e}{2} (1 - \|\Lambda_e\|_2^2) \cdot x_e (g_e(\|\Lambda_e\|_2) - 1) \leq 0,$$

where the inequality holds since $g_e(\|\Lambda_e\|_2) - 1$ and $\|\Lambda_e\|_2 - 1$ have the same sign, as g_e is a non-negative and increasing function with $g_e(1) = 1$.

We have equality if and only if for all e either $x_e = 0$ or $\Lambda_e = 1$. Thus $x \in \mathcal{V}$ if and only if $x \in \mathcal{F}_g$. \square

7 Further Properties of the Lyapunov Minimum

We give two alternative characterizations for the minimum of the Lyapunov function. This extends [FCP18, Proposition 2] from $k = 1$ to arbitrary k .

Theorem 5. *The following quantities $MinQ$, $MaxP$, and $MinL$ are equal.*

$$MinQ = \min_{Q \in \mathbb{R}^{m \times k}} \left\{ \sum_e c_e \|Q_e\|_2 : AQ = B \right\}, \quad (11)$$

$$MaxP = \max_{P \in \mathbb{R}^{n \times k}} \{ \text{Tr}[B^T P] : \|A_e^T P\|_2 \leq c_e \text{ for all } e \}, \quad (12)$$

$$MinL = \min_{x \in \mathbb{R}_{\geq 0}^m} \mathcal{L}(x). \quad (13)$$

Moreover, there are optimizers Q^* , P^* and x^* such that

$$\begin{aligned} x_e^* &= \|Q_e^*\|_2 \quad \text{for all } e, \\ L(x^*)P^* &= B, \\ Q^* &= X^* C^{-1} A^T P^*. \end{aligned}$$

It is instructive to interpret the theorem for the case $k = 1$, A the node-arc incidence matrix of a directed graph, and b a vector with one entry $+1$ and one entry -1 and all other entries equal to zero. Then $MinQ = \min_{q \in \mathbb{R}^m} \{ \sum_e c_e |q_e| : Aq = b \}$ is the minimum cost of a flow realizing b in the underlying undirected network and $MaxP = \max_{p \in \mathbb{R}^n} \{ b^T p : |p_v - p_u| \leq c_e \text{ for all } e = (u, v) \}$ is the maximum distance between the two nodes designated by b for any distance function on the nodes satisfying the length constraints imposed by c . Clearly, $MinQ = MaxP$. The third characterization via $MinL = \min_{x \geq 0} \mathcal{L}(x)$ is non-standard. Note that $\mathcal{L}(x) = (c^T x + b^T p)/2$, where p are node potentials driving a current of 1 between the nodes designated by b in the network with edge resistances c_e/x_e . Then $b^T p$ is the potential difference between the two designated nodes which, since the driven current is one, is the effective resistance between the two designated nodes. In Lemma 8, we determined $\frac{\partial}{\partial x_e} \mathcal{L}(x) = \frac{c_e}{2} (1 - \|\Lambda_e\|_2^2)$, i.e., the minimizer x^* of $\mathcal{L}(x)$ must satisfy $x_e^* \neq 0 \Rightarrow |A_e^T p^*| = c_e$, where p^* are node potentials corresponding to x^* . Note that for an edge $e = (u, v)$, $|A_e p^*| = |p_v^* - p_u^*|$ is the potential drop on e . Orient all edges such that potential drops are positive and consider any path W (W for Weg) in $\text{supp}(x^*)$ connecting the two designated nodes. Then

$$b^T p^* = \sum_{e \in W} A_e^T p^* = \sum_{e \in W} c_e,$$

since the potential difference between the two designated nodes is the sum of the potential drops along W . Thus any two paths in $\text{supp}(x^*)$ connecting the two designated nodes must have the

same cost and hence (assuming that any two such paths have distinct cost) $\text{supp}(x^*)$ contains a single path connecting the two designated nodes. In fact, $\text{supp}(x^*)$ is equal to such a path. Now $\sum_{e \in W} c_e x_e + \sum_{e \in W} c_e/x_e = \sum_{e \in W} (c_e x_e + c_e/x_e)$ is minimized for $x_e = 1$ for all $e \in W$ and then is equal to twice the cost of W . Of course, the cost of W is minimized for the shortest undirected path connecting the two designated nodes.

Lemma 9. *Let Q^* be a minimizer of (11) and let x^* be defined by $x_e^* = \|Q_e^*\|_2$ for all e . Then $x^* \in \mathcal{F}_g$. Moreover, there is a potential matrix $P \in \mathbb{R}^{n \times k}$ such that $L(x^*)P = B$ and $Q = X^*C^{-1}A^T P$, $\sum_e c_e \|Q_e\|_2 = \text{Tr}[B^T P] = \mathcal{L}(x^*)$, and $\|A_e^T P\|_2 \leq c_e$ for all e . The objective values of (11) to (13) satisfy $\text{Min}L \leq \text{Min}Q \leq \text{Max}P$.*

Proof. We start by slightly reformulating the minimization problem (11). This is necessary since the function $Q_e \mapsto \|Q_e\|_2$ is not differentiable for $Q_e = 0$ and hence the KKT-conditions cannot be applied. We formulate equivalently:

$$\min \sum_e c_e x_e \text{ subject to } AQ = B, x_e^2 \geq \|Q_e\|_2^2, x_e \geq 0 \text{ for all } e,$$

with variables $Q \in \mathbb{R}^{m \times k}$ and $x \in \mathbb{R}^m$. Let Q^* and x^* be an optimal solution. Then clearly $x_e^* = \|Q_e^*\|_2$ for all e . Using the Lagrange multipliers $P \in \mathbb{R}^{n \times k}$ for the equations $AQ = B$, and $\alpha \in \mathbb{R}_{\geq 0}^m$ and $\beta \in \mathbb{R}_{\geq 0}^m$ for the inequalities, the KKT conditions [BV04, Subsection 5.5] become

$$c_e - 2\alpha_e x_e - \beta_e = 0 \quad \text{for all } e, \quad (14)$$

$$P_i^T A_e + 2\alpha_e Q_{e,i}^* = 0 \quad \text{for all } e \text{ and } i, \quad (15)$$

$$\alpha_e (x_e^2 - \|Q_e^*\|_2^2) = 0 \quad \text{for all } e, \quad (16)$$

$$\beta_e x_e = 0 \quad \text{for all } e. \quad (17)$$

Here the first two conditions state that at the optimum, the gradient of the objective with respect to the variables x_e and Q_{ei} must be linear combinations of the gradients of the active constraints and the last two conditions are complementary slackness (= a Lagrange multiplier can only be non-zero if the constraint is tight). We also have the feasibility constraints

$$AQ_i^* = b_i \quad \text{for all } i, \quad (18)$$

$$x_e^* \geq 0 \text{ and } x_e^* \geq \|Q_e\|_2 \quad \text{for all } e. \quad (19)$$

Separating the two terms in (15), squaring and summing over i , and using (15) and (14), we obtain

$$\|A_e^T P\|_2^2 = \sum_i (P_i^T A_e)^2 = 4\alpha_e^2 \|Q_e^*\|_2^2 = 4\alpha_e^2 (x_e^*)^2 = (c_e - \beta_e)^2 \leq c_e^2,$$

where the last inequality uses $\beta_e = 0$ if $x_e > 0$ by (17) and $\beta_e = c_e$ if $x_e = 0$ by (14).

If $Q_e^* \neq 0$, then $x_e^* \neq 0$ and hence $\beta_e = 0$ and $c_e = 2\alpha_e x_e^*$ or $2\alpha_e = c_e/x_e^*$. In particular, $\alpha_e \neq 0$ and hence (15) implies

$$Q_{e,i}^* = \frac{1}{2\alpha_e} \sum_v P_{v,i} A_{v,e} = \frac{x_e^*}{c_e} A_e^T P_i. \quad (20)$$

This equation also holds if $Q_e^* = 0$ and hence $x_e^* = 0$. Multiplying by A_e from the left and summing over e yields

$$b_i = AQ_i^* = \sum_e A_e \frac{x_e^*}{c_e} A_e^T P_i = AX^*C^{-1}A^T P_i. \quad (21)$$

Thus P_i is a potential for the i -th problem with respect to x^* and, by (20) Q_i^* is the corresponding

electrical flow. Thus $x^* \in \mathcal{F}_g$ by Lemma 2. Moreover,

$$\begin{aligned}
\sum_i P_i^T b_i &= \sum_i P_i^T A Q_i^* \\
&= \sum_{i,v,e} P_{v,i} A_{v,e} Q_{e,i}^* \\
&= \sum_{i,v,e, Q_e \neq 0} P_{v,i} A_{v,e} Q_{e,i}^* \\
&= \sum_{i,e, Q_e \neq 0} c_e \frac{Q_{e,i}^* Q_{e,i}^*}{\|Q_e^*\|_2} \\
&= \sum_e c_e \|Q_e^*\|_2.
\end{aligned}$$

Here the fourth equality comes from (20) and $x_e^* \neq 0$ if $Q_e^* \neq 0$; note that

$$\sum_v A_{ve} P_{vi} = A_e^T P_i = \frac{c_e}{x_e^*} Q_{ei}^* = c_e \frac{Q_{ei}^*}{\|Q_e^*\|_2}.$$

We conclude that P is a feasible solution to (12). Thus $MaxP \geq MinQ$.

Since $x^* \in \mathcal{F}_g$, $\mathcal{L}(x^*) = c^T x^* = \text{Tr}[P^T L(x^*) P]$. Also, $x_e^* = \|Q_e^*\|_2$ by definition of x^* . Thus

$$\sum_e c_e \|Q_e^*\|_2 = c^T x^* = \mathcal{L}(x^*)$$

and hence $MinL \leq MinQ$. □

Lemma 10. $MaxP \leq MinL$.

Proof. The constraint $\|A_e^T P\|_2 \leq c_e$ in (12) can be equivalently written as

$$\frac{c_e}{2} \left(\left\| \frac{1}{c_e} A_e^T P \right\|_2^2 - 1 \right) \leq 0.$$

Then the Lagrange dual with non-negative multipliers x_e is an upper bound for $MaxP$, i.e.,

$$MaxP \leq \inf_{x \geq 0} \sup_P \sum_i b_i^T P_i - \sum_e \frac{x_e c_e}{2} \left(\left\| \frac{1}{c_e} A_e^T P \right\|_2^2 - 1 \right).$$

The inner supremum can be reformulated as

$$\sup_P \sum_i b_i^T P_i - \frac{1}{2} \sum_i P_i^T L(x) P_i + \frac{1}{2} c^T x, \quad (22)$$

since $(x_e/c_e) \sum_i (A_e^T P_i)^2 = \sum_i P_i^T A_e (x_e/c_e) A_e^T P_i$. Only the first two terms in (22) depend on P . We want to determine the maximizer⁵ $P(x)$. Taking partial derivatives with respect to the vectors P_i leads to the system

$$A X C^{-1} A \cdot P_i(x) = b_i \quad \text{for all } i,$$

i.e. $P_i(x)$ is a solution to $L(x) P_i(x) = b_i$ for each i . Since

$$\sum_i b_i^T P_i(x) = \text{Tr}[B^T P(x)] = \text{Tr}[P(x)^T L(x) P(x)] = \sum_i P_i(x)^T L(x) P_i(x)$$

substituting into (22) yields

$$\sup_P \sum_i b_i^T P_i - \frac{1}{2} \sum_i P_i^T L(x) P_i + \frac{1}{2} c^T x = \frac{1}{2} (\text{Tr}[B^T P(x)] + c^T x) = \mathcal{L}(x).$$

□

⁵In the proof of Lemma 3, we have seen that $L(x) = A D^{1/2} D^{1/2} A^T$ and hence $b_i^T P_i - P_i^T L(x) P_i = b_i^T P_i - \|D^{1/2} A^T P_i\|_2^2$. Thus the maximizer is a finite point.

Lemma 11. *Let $x^* \in \mathbb{R}_{\geq 0}^m$ be a minimizer of $\mathcal{L}(x)$. Then $x^* \in \mathcal{F}_g$. Let P be a solution to $L(x)P = B$ and let $Q = X^*C^{-1}A^TP$. Then $\sum_e c_e \|Q_e\|_2 = \mathcal{L}(x^*)$ and hence $\text{Min}Q \leq \text{Min}L$.*

Proof. Since $\mathcal{L}(x(t))$ is a Lyapunov function of the generalized Physarum dynamics we have $x^* \in \mathcal{V}$. Since $\mathcal{V} = \mathcal{F}_g$, x^* is a fixed point and hence for all e , either $x_e^* = 0$ or $\Lambda_e = 1$. Since x^* is a fixed point, we have $\mathcal{L}(x^*) = c^T x^* = \text{Tr}[P^T L(x^*)P]$ and $x_e^* = \|Q_e\|_2$ for all e . Thus

$$\sum_e c_e \|Q_e\|_2 = c^T x^* = \mathcal{L}(x^*)$$

and hence $\text{Min}Q \leq \text{Min}L$. □

8 Convergence to the Lyapunov Minimizer

We show that the dynamics converges to the minimizer x^* of the Lyapunov function under the assumption that the set of fixed points of the dynamics is a discrete set.

Assumption 2 (Discrete Set of Fixed Points). *\mathcal{F}_g is a finite set of points. For any two points in \mathcal{F}_g , the values of \mathcal{L} are distinct.*

Theorem 6. *Let $x^* = \text{argmin}_{x \geq 0} \mathcal{L}(x)$. Under the additional assumption 2, the generalized Physarum dynamics $x(t)$ converges to x^* .*

Proof. Since $\mathcal{L}(x(t))$ is non-increasing and non-negative, the dynamics $x(t)$ converges to the set \mathcal{V} . By Theorem 4, $\mathcal{V} = \mathcal{F}_g$. Since \mathcal{F}_g is assumed to be a finite set and any two fixed points have distinct values of \mathcal{L} , there is a fixed point $\hat{x} = \lim_{t \rightarrow \infty} x(t)$. Assume for the sake of a contradiction, $\mathcal{L}(\hat{x}) > \mathcal{L}(x^*)$. Let $P(t)$ be the node potential corresponding to $x(t)$ and let \hat{P} be the potential corresponding to \hat{x} ; recall that node potentials are unique. Since $P(t)$ is a continuous function of $x(t)$, $P(t) \rightarrow \hat{P}$ as $t \rightarrow \infty$. Let $\hat{E} = \{e : \|A_e^T \hat{P}\|_2 \leq c_e\} \subseteq E$ and consider the following chain of inequalities:

$$\begin{aligned} \max_P \left\{ \text{Tr}[B^T P] : \|A_e P\|_2 \leq c_e \text{ for all } e \in \hat{E} \right\} &\geq \text{Tr}[B^T \hat{P}] \\ &= \mathcal{L}(\hat{x}) \\ &> \mathcal{L}(x^*) \\ &= \max_P \left\{ \text{Tr}[B^T P] : \|A_e P\|_2 \leq c_e \text{ for all } e \in E \right\}, \end{aligned}$$

where the first inequality follows by the definition of \hat{E} , the first equality follows from Lemma 2, the strict inequality holds by assumption and the last equality follows from Theorem 5. We conclude that \hat{E} is a proper subset of E .

Let $e \in E \setminus \hat{E}$ be arbitrary. Then $\|A_e^T \hat{P}\|_2 > c_e$ and hence there are $t_0 > 0$ and $\varepsilon > 0$ such that for every $t \geq t_0$ we have

$$\|\Lambda_e(t)\|_2 = \frac{\|A_e^T P(t)\|_2}{c_e} > 1 + \varepsilon.$$

Since g_e is an increasing function with $g_e(1) = 1$, there is $\alpha > 0$ such that

$$g_e(\|\Lambda_e(t)\|_2) \geq g_e(1 + \varepsilon) = 1 + \alpha.$$

Then, for the generalized dynamics we have

$$\dot{x}_e(t) = x_e(t) \cdot (g_e(\|\Lambda_e(t)\|_2) - 1) \geq x_e(t) \cdot (g_e(1 + \varepsilon) - 1) \geq \alpha x_e(t).$$

Further, by Gronwall's Lemma, it follows that

$$x_e(t) \geq x_e(t_0) \cdot e^{\alpha t},$$

and thus

$$\hat{x}_e = \lim_{t \rightarrow \infty} x_e(t) \geq x_e(t_0) \cdot \lim_{t \rightarrow \infty} e^{\alpha t} = +\infty.$$

This is a contradiction to the fact that \hat{x}_e is bounded.

Finally, if $\mathcal{L}(x(t))$ converges to $\min_{x \geq 0} \mathcal{L}(x)$ and the minimizer x^* of \mathcal{L} is unique, then $x(t)$ must converge to x^* . \square

We conjecture that $x(t)$ always converges to some minimizer of \mathcal{L} . If there are several minimizers of \mathcal{L} , the limit depends on the initial configuration and the function g . Consider the following simple example. We have a network with two nodes connected by two links of the same cost, $k = 1$ and the goal is to send one unit between the two nodes. Let x_1 and x_2 be the capacities of the two links, respectively. For $g(z) = z$, any combination (x_1, x_2) with $x_1 + x_2 = 1$ is a fixed point.

9 A Connection to Mirror Descent

We show that the *mirror descent* dynamics on the Lyapunov function \mathcal{L} is equal to a variant of the non-uniform squared Physarum dynamics.

Lemma 12. *The dynamics*

$$\frac{d}{dt} x_e(t) = \frac{c_e}{2} x_e(t) (\|\Lambda_e\|_2^2 - 1)$$

is equivalent to the mirror descent dynamics on the Lyapunov function \mathcal{L} .

Proof. By Lemma 8, we have for every index $e \in E$ that

$$\frac{\partial}{\partial x_e} \mathcal{L}(x) = \frac{c_e}{2} (1 - \|\Lambda_e\|_2^2). \quad (23)$$

On the other hand, the mirror descent dynamics on the Lyapunov function \mathcal{L} is given by

$$\frac{d}{dt} x_e(t) = -x_e(t) \frac{\partial}{\partial x_e} \mathcal{L}(x_e(t)) \stackrel{(23)}{=} \frac{c_e}{2} \cdot x_e(t) (\|\Lambda_e\|_2^2 - 1). \quad \square$$

As is [Bon19], we can use the connection to mirror descent to estimate the speed of convergence of the Physarum dynamics to the Lyapunov minimum; [Bon19] builds up on [ABB04, Wil18].

For a differentiable function f in m variables, the Bregman divergence D_f is a function in $2m$ variables defined by the equation

$$D_f(x, y) = f(x) - f(y) - \langle \nabla f(y), x - y \rangle,$$

i.e., as the difference of the function value at x and the value at x of the tangent plane to f at y . Clearly, if f is convex, D_f is non-negative.

Lemma 13. *Let $h : \mathbb{R}_{\geq 0}^m \rightarrow \mathbb{R}$ be defined by*

$$h(x) = \sum_e x_e \ln x_e - \sum_e x_e.$$

Then h is convex on $\mathbb{R}_{\geq 0}^m$, D_h is non-negative, and

$$D_h(x, y) = \sum_e x_e \ln x_e - \sum_e x_e \ln y_e - \sum_e x_e + \sum_e y_e,$$

Proof. The function h is convex in x_e (partial derivative $\ln x_e$ and second partial derivative $1/x_e$). For its Bregman divergence D_h , we compute

$$\begin{aligned} D_h(x, y) &= h(x) - h(y) - \langle \nabla h(y), x - y \rangle \\ &= \sum_e x_e \ln x_e - \sum_e x_e - \left(\sum_e y_e \ln y_e - \sum_e y_e \right) - \sum_e (x_e - y_e) \ln y_e \\ &= \sum_e x_e \ln x_e - \sum_e x_e \ln y_e - \sum_e x_e + \sum_e y_e. \end{aligned}$$

So D_h is the *relative entropy* function. □

Fact 1. [Bon19, Lemma 2.2] \mathcal{L} is convex.

Theorem 7. Let x^* be the global minimizer of $\mathcal{L}(x)$. For the dynamics $\dot{x}_e = (c_e/2) \cdot x_e (\|\Lambda_e\|_2^2 - 1)$, we have

$$\mathcal{L}(x(t)) \leq \mathcal{L}(x^*) + \frac{1}{t} D_h(x^*, x(0)).$$

for all $t \geq 0$. In particular,

$$\lim_{t \rightarrow \infty} \mathcal{L}(x(t)) = \mathcal{L}(x^*).$$

Proof. According to (23) we have

$$\frac{\partial}{\partial x_e} \mathcal{L}(x) = \frac{c_e}{2} (1 - \|\Lambda_e\|_2^2) \quad \text{and} \quad \dot{x}_e = x_e (g_e(\|\Lambda_e\|_2^2) - 1).$$

The time derivative of $D_h(x^*, x(t))$ is given by

$$\begin{aligned} \frac{d}{dt} D_h(x^*, x) &= \frac{d}{dt} \sum_{e=1}^m x_e^* \ln x_e^* - \frac{d}{dt} \sum_e x_e^* \ln x_e - \frac{d}{dt} \sum_e x_e^* + \frac{d}{dt} \sum_e x_e \\ &= \sum_{e=1}^m x_e^* \left(-\frac{1}{x_e} \cdot \frac{d}{dt} x_e \right) + \sum_e \frac{d}{dt} x_e \\ &= \sum_e (x_e - x_e^*) \frac{c_e}{2} (\|\Lambda_e\|_2^2 - 1) \\ &= -\langle (x - x^*), \nabla \mathcal{L}(x(t)) \rangle. \end{aligned}$$

We now consider the function

$$\mathcal{H}(t) = D_h(x^*, x(t)) + t [\mathcal{L}(x(t)) - \mathcal{L}(x^*)]$$

Since $\frac{d}{dt} \mathcal{L}(x) \leq 0$, by Lemma 4, and $D_{\mathcal{L}}(x^*, x) \geq 0$ for all x , we obtain

$$\begin{aligned} \frac{d}{dt} \mathcal{H}(t) &= -\langle \nabla \mathcal{L}(x(t)), x(t) - x^* \rangle + \mathcal{L}(x(t)) - \mathcal{L}(x^*) + t \cdot \frac{d}{dt} \mathcal{L}(x(t)) \\ &\leq -[\mathcal{L}(x^*) - \mathcal{L}(x(t)) - \langle \nabla \mathcal{L}(x), x^* - x(t) \rangle] \\ &= -D_{\mathcal{L}}(x^*, x(t)) \\ &\leq 0. \end{aligned}$$

Hence $\mathcal{H}(t) \leq \mathcal{H}(0)$ for all $t \geq 0$ and therefore

$$D_h(x^*, x(t)) + t [\mathcal{L}(x(t)) - \mathcal{L}(x^*)] \leq D_h(x^*, x(0)) + 0 [\mathcal{L}(x(0)) - \mathcal{L}(x^*)].$$

and further (using $D_h(x^*, x(t)) \geq 0$)

$$\mathcal{L}(x(t)) \leq \mathcal{L}(x^*) + \frac{1}{t} D_h(x^*, x(0)).$$

□

10 Conclusions

We proposed a variant of the Physarum dynamics suitable for network design. We exhibited a Lyapunov function for the dynamics, proved convergence of the dynamics, and gave alternative characterizations for the minimum of the Lyapunov function. In the experiment part, we showed that the dynamics captures the positive effect of sharing links and is able to construct *nice* networks.

Many questions remain open. We do not claim any biological plausibility for our proposal. It would be very interesting to define a dynamics which is biologically plausible. We used an Euler discretization of the dynamics for the experiments in Section 2. The resulting algorithm is quite slow. The Lyapunov function \mathcal{L} is a convex function and hence the tool box of convex optimization is available for computing its minimum. Does this lead to a practical algorithm for network design?

References

- [ABB04] F. Alvarez, J. Bolte, and O. Brahic. Hessian Riemannian gradient flows in convex programming. *SIAM J. Control and Optimization*, 43(2):477501, 2004.
- [BBK⁺19] Ruben Becker, Vincenzo Bonifaci, Andreas Karrenbauer, Pavel Kolev, and Kurt Mehlhorn. Two Results on Slime Mold Computations. *Theoretical Computer Science*, 773:79–106, 2019.
- [BD97] S. L. Baldauf and W. F. Doolittle. Origin and evolution of the slime molds (Mycetozoa). *Proc. Natl. Acad. Sci. USA*, pages 12007–12012, 1997.
- [BMV12] Vincenzo Bonifaci, Kurt Mehlhorn, and Girish Varma. Physarum can compute shortest paths. *Journal of Theoretical Biology*, 309(0):121–133, 2012. A preliminary version of this paper appeared at SODA 2012 (pages 233-240).
- [Bon13] Vincenzo Bonifaci. Physarum can compute shortest paths: A short proof. *Inf. Process. Lett.*, 113(1-2):4–7, 2013.
- [Bon16] Vincenzo Bonifaci. A revised model of fluid transport optimization in Physarum polycephalum. *Journal of Mathematical Biology*, 74:567–581, 2016.
- [Bon19] Vincenzo Bonifaci. A Laplacian approach to ℓ_1 -norm minimization. *CoRR*, abs/1901.08836, 2019.
- [BV04] Stephen Boyd and Lieven Vandenberghe. *Convex Optimization*. Cambridge University Press, 2004.
- [FCP18] E. Facca, F. Cardin, and M. Putti. Physarum dynamics and optimal transport for basis pursuit. *arXiv:1812.11782 [math.NA]*, December 2018.
- [FDCP18] E. Facca, S. Daneri, F. Cardin, and M. Putti. Numerical solution of Monge-Kantorovich equations via a dynamic formulation. *arXiv:1709.06765 [math.NA]*, 2018.
- [Har02] P. Hartman. *Ordinary Differential Equations: Second Edition*. SIAM, 2002.
- [IJNT11] Kentaro Ito, Anders Johansson, Toshiyuki Nakagaki, and Atsushi Tero. Convergence properties for the Physarum solver. *arXiv:1101.5249v1*, January 2011.
- [KKM20] Andreas Karrenbauer, Pavel Kolev, and Kurt Mehlhorn. Convergence of the Non-Uniform Physarum Dynamics. *Theor. Comput. Sci.*, 816:260–269, 2020.
- [NYT00] T. Nakagaki, H. Yamada, and Á. Tóth. Maze-solving by an amoeboid organism. *Nature*, 407:470, 2000.

- [SV16a] Damian Straszak and Nisheeth K. Vishnoi. IRLS and slime mold: Equivalence and convergence. *CoRR*, abs/1601.02712, 2016.
- [SV16b] Damian Straszak and Nisheeth K. Vishnoi. On a natural dynamics for linear programming. In *ITCS*, pages 291–291, New York, NY, USA, 2016. ACM.
- [TKN07] A. Tero, R. Kobayashi, and T. Nakagaki. A mathematical model for adaptive transport network in path finding by true slime mold. *Journal of Theoretical Biology*, pages 553–564, 2007.
- [TTS⁺10] A. Tero, S. Takagi, T. Saigusa, K. Ito, D. Bebbler, M. Fricker, K. Yumiki, R. Kobayashi, and T. Nakagaki. Rules for biologically inspired adaptive network design. *Science*, 327:439–442, 2010.
- [Wil18] A. Wilson. *Lyapunov arguments in optimization*. PhD thesis, University of California at Berkeley, 2018.